A comparison of microstructure and of thermal transport properties of yttria and ceria stabilized zirconia coatings deposited by suspension plasma spraying

Pawel Sokolowski, Leszek Latka, Stefan Kozerski, Andrzej Ambroziak, Lech Pawlowski, Bernard Pateyron

A comparison of microstructure and of thermal transport properties of yttria and ceria stabilized zirconia coatings deposited by suspension plasma spraying

Sokołowski P., Łatka L., Kozerski S., Ambroziak A.. Wroclaw University of Technology, Wroclaw / PL
Pawłowski L., Pateyron B., University of Limoges, Limoges / FR

The single cathode plasma torch SG-100 was used to spray suspension prepared with the use of two kinds of commercial powders ZrO_2+8 wt. % Y_2O_3 (8YSZ) and ZrO_2 + 24 wt.% CeO_2 + 2.5 wt.% Y_2O_3 (24CeYSZ). The suspensions were formulated using finely milled solid phase, water and ethanol. The operational spray parameters being the same for each powder were modified by changing: (i) spray distance; and (ii) torch scan linear speed. The coatings microstructures were analyzed with the use of optical and scanning electron microscopes as well as by X-ray diffraction. Their porosities were found with help of the image analysis of metallographically prepared cross-sections. Thermal diffusivity was measured with the use of commercial system LFA 447 NanoFlash® working at the temperatures limited to 300°C. The measurements were made with the use of the coatings sprayed on the steel substrate and a 2-layers numerical model was applied to determine thermal diffusity of the coatings. The obtained data were used to calculate thermal conductivity of stabilized zirconia coatings.

1 Introduction

Suspension Plasma Spraying (SPS) is one of relatively new methods and is currently very frequently tested to apply the oxide coatings. It was initiated a by the end of last century (in 1997) by the group of researchers from Sherbrooke University in Canada [1]. The innovation of the presented method was the use the feedstock being the suspension of fine solids. However, the use of liquid feedstock instead of dry one, resulted in a change of the processes which became more complex than the standard plasma spraying [2].
During the spraying process such physical effects as: evaporation of liquid part of suspension's, in-flight agglomeration and sintering of solids, their melting and vaporization or splats formation on the surface of the element may occur [3,4]. Moreover, the optimal process variables including size and properties of solid phase, spray process parameters, type of the plasma torch and injection mode are not easy to find out. Consquently, the optimization of spray parameters is more difficult in the SPS method in in conventional plasma spraying. On the other hand, the suspension plasma spraying enables obtaining the coatings having finely grained microstructure with very interesting properties. In particular, thermal conductivity of yttria or ceria stabilized zirconia coatings seems to be considerably lower than that obtained by the use of conventional feedstock [5]. For this reason The SPS coatings are considered to be used as thermal barrier coatings (TBCs) in gas turbines.
The presented experiments were undertaken to characterize microstructure and thermal transport properties of coatings obtained with the use of fine, submicrometric zirconia powders and different spray parameters. The research was carried out aiming the comparison the different properties of zirconia coatings stabilized with different oxides. Finally, the studies allowed evaluating the possibilities of producing TBC with the suspension plasma spraying method.

2 Experimental procedures

2.1 Powders and suspensions preparation

Two commercial powders, namely Metco 204NS having composition ZrO_2 + 8 wt. % Y_2O_3 and Metco 205NS having composition ZrO_2 + 24 wt.% CeO_2 + 2.5 wt. % Y_2O_3 were used to spray the coatings. The mean diameters of initial, coarse powders were the same and equal to d_{vs}=38µm. The morphology of powders is presented in Fig. 1.

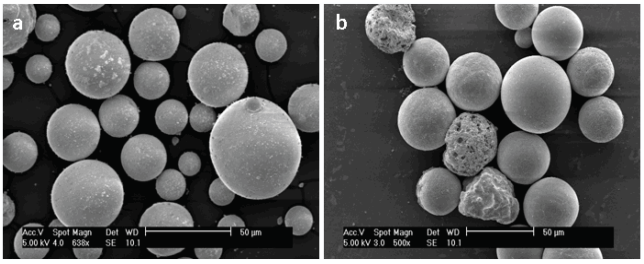

Fig. 1 SEM image (secondary electrons) showing the morphology of commercial (a) 204NS and (b) 205NS powders.

The initial powders were ball-milled in order to obtain finer particles. The ball-milling was made using moliNEx system (NETZSCH, Germany). The zirconia balls with the diameter of about 2mm were used as grinding medium and a small addition of ethanol as cooling one. Small addition of the dispersant (Beycostat C213, CECA) was used prevent agglomeration of particles during milling process. The granulometry tests were made based on the laser diffraction analysis (Partica LA-950V2, Horiba). The measurements showed that the resulting powder after 2h of milling had a mean size equal to: d_{vs}=4.5 µm (8YSZ) and d_{vs}=3.9 µm (24CeYSZ) (Fig.2.) and a monomodal size distribution.

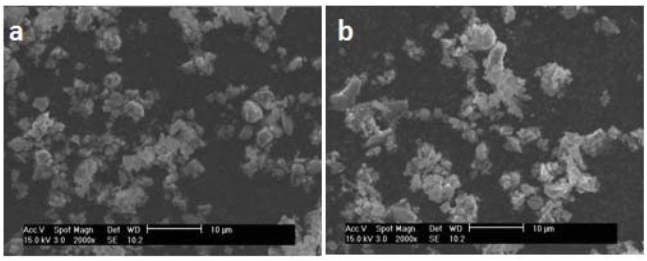

Fig. 2 SEM photo (secondary electrons) of 8YSZ and 24CeYSZ powders after milling process

The suspension were prepared from the mixtures of 20 wt. % of solid, 40 wt. % of water and 40 wt. % of ethanol. The zeta potential of suspensions was measured using Zetasizer Nano ZS (Malvern, UK). The suspensions were not stable and dispersant agent was added (Beycostat C213, CECA) to avoid agglomeration of particles. The resulting zeta potential was as low as ζ = -8.6 mV for 8YSZ powder suspension and ζ = -6,2 mV for 24CeYSZ. The entire procedure of preparation of powders and suspensions is described in [6].

2.2 Design of spray process experiments

The spray process was realized using an SG-100, DC single cathode and single anode torch of Praxair S.T., (Indianapolis, USA). Plasma torch was installed on a 5-axis IRB-6 industrial robot of ABB (Zürich, Switzerland).The experiment was designed by two-level full factorial design (2^k) with k=2 in which the variable parameters were: (i) torch scan velocity (300 and 500 mm/s); and (ii) spray distance (40 and 60 mm). Other important parameters of the process were kept constant, namely electric power equal to 40 kW, working gases composition was Ar – 45 slpm with H_2 – 5 slpm and suspension feed rate was about 39 g/min. The coatings surface temperatures measured at spray experiments are presented in Table 1.

Table 1 Spraying parameters and coatings surface temperature

Run	Scan velocity [mm/s]	Spray dist. [mm]	Max. surface temp. 24YSZ [°C]	Max. surface temp. 24CeYSZ [°C]
1	300	40	570 – 690	670 – 740
2	500	40	490 – 650	510 – 640
3	400	50	460 – 530	450 – 600
4	300	60	410 – 570	420– 560
5	500	60	380 – 460	390– 470

The stainless steel samples of O.D.=25 mm and thickness of 3 mm were used as substrates. The substrates were sand blasted using 500 µm white alumina sand and cleaned in ethanol before deposition. The temperature of the top surface of the samples was controlled with the use of the pyrometer during spraying. In order to avoid the overheating of the substrates the process was interrupted after every three scans of the torch and the samples were cooled down by compressed air.

2.3 Microstructure characterization

The scanning electron microscope (Jeol JSM-7400) was used to characterize powders and another one (Philips 515) was used to characterize the coatings. The phase composition of coatings was determined with X-ray diffractometer (Bruker D8 Advance) with CuKα1 radiation and a range of 2θ angles from 15° to 120°. The pahses were identified using Diffrac+ Eva software.
The coatings porosities and thicknesses were characterized with use of optical microscope (Nikon LV100). The cross-sections of samples were metallographically prepared. The thicknesses of coating was found from 5 measurements in 3 different regions of samples. The porosity was found using image analyzer working with ImageJ software [7].

2.4 Thermal diffusivity measurements

Thermal diffusivity was measured with the use of commercial system LFA 447 NanoFlash®, Netzsch. The samples were coated on each face with graphite layer before measurement to provide better propagation of heat and to allow reading of small temperature changes by the detector. The signals were measured with InSb infrared detector. The model used initially to determine thermal diffusivity by flash laser set up for homogenous samples is Cowan model [8]. The multilayer materials require more complex methods of calculation. The analysis of thermal diffusivity was made with the use of 2-layers model with finite pulse duration correction. Thermal contact resistance between the layers and heat losses were also taken into account. The measurements enabled to find the thermal diffusivity of coatings. Other properties of tested samples, such as density ρ, heat capacity c_p, material and thermal diffusivity of the steel substrate were taken from literature (Table 2) [9-12]. The thickness of coating and substrate were measured experimentally. The following equation was used to calculate thermal conductivity of 8YSZ and 24CeYSZ coatings:

$$\lambda(T) = a(T) \cdot c_p(T) \cdot \frac{\rho_{300}}{1+3\cdot\frac{\Delta L}{L}(T)} \qquad (1)$$

where:
λ – thermal conductivity [W/(m·K)]
a – thermal diffusivity [m^2/s]
c_p – specific heat [J/(kg·K)]
ρ_{300} – apparent density in ambient temperature [kg/m^3]
$\frac{\Delta L}{L}$ – thermal dilatation [–]

The entire procedure of collecting the material properties has been thoroughly described in previous studies of the authors [11, 12]. The data used in present study are presented in Table 2 and Table 3.

Table 2 Thermal dilatation and specific heat values for 8YSZ and 24CeYSZ coatings [9, 10]

Temperature T [K]	Specific heat c_p of YSZ [J/(kg·K)]	Specific heat c_p of YCSZ [J/(kg·K)]	Thermal dilatation $\frac{\Delta L}{L}$ [–]
298	438	427	$4.2606.10^{-5}$
323	453	441	$2.5646.10^{-4}$
373	480	465	$6.8840.10^{-4}$
423	501	485	$1.1262.10^{-3}$
473	518	501	$1.5702.10^{-3}$
523	531	514	$2.0206.10^{-3}$

3 Results

3.1 Microstructure description

The micrographs of coatings surfaces and their cross-sections of 8YSZ and 24CeYSZ coatings showed typical *two-zones* microstructure of the suspension plasma spraying method in which occur well molten lamella and very fine spherical particles (see e.g. Fig.3a). The 24CeYSZ coatings microstructure shows a bit more of fine particles and less of well-molten big splats than that of 8YSZ ones (compare Figs 3 a and Fig. 3 c). The SEM images of the cross-sections of 8YSZ coatings (Fig.3b) showed also well molten lamellae and some pores, which have been formed between them, while the cross-sections of 24CeYSZ coatings (Fig.3d) were characterized by greater number of pores and microcracks.
The phase analysis determined by X-ray diffraction revealed that the major phase for both YSZ and YCSZ were tetragonal zirconia with a small addition of monoclinic phase. The results of phase composition are collected also in Table 3.

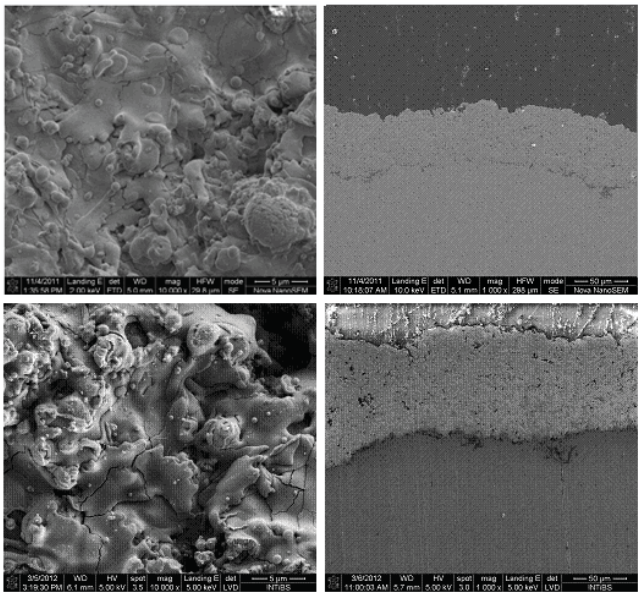

Fig. 3. SEM images (secondary electrons) showing (a) top surface of 8YSZ coating, (b) cross-section of 8YSZ coating, (c) top surface of 24CeYSZ coating and (d) cross-section of 24CeYSZ coating

3.2 Thermal diffusivity

Thermal diffusivity data for 8YSZ and 24CeYSZ coatings are presented in Fig. 4. Thermal diffusivity values for samples of 8YSZ coatings were in the range from 0.20 to $0.35x10^{-6}$ m^2/s depending on the spray run (Fig.4a). The coatings obtained in the run no. 2 have the greatest diffusivity and the samples in the run no. 4 – the lowest. In the case of 24CeYSZ coatings, diffusivity values were in the range of 0.23 to $0.49x10^{-6}$ m^2/s. As it can be seen, the samples sprayed in the run no. 2 have the greatest diffusivity, while the samples sprayed in the run no. 1 have the lowest one (Fig.4b).

Table 3 Results of microstructure characterization [6, 11]

Run	Thickness of 8YSZ [µm]	Thickness of 24CeYSZ [µm]	Porosity of 8YSZ [%]	Porosity of 24CeYSZ [%]	Tetragonal ZrO_2 in 8YSZ [%]	Tetragonal ZrO_2 in 24VeYSZ [%]
1	100	53	9	21.5	89.2	95.0
2	106	90	8	18.7	90.4	96.1
3	54	78	9	20.3	91.6	95.9
4	51	101	10	15.1	92.6	95.4
5	60	88	12	20.6	92.9	95.9

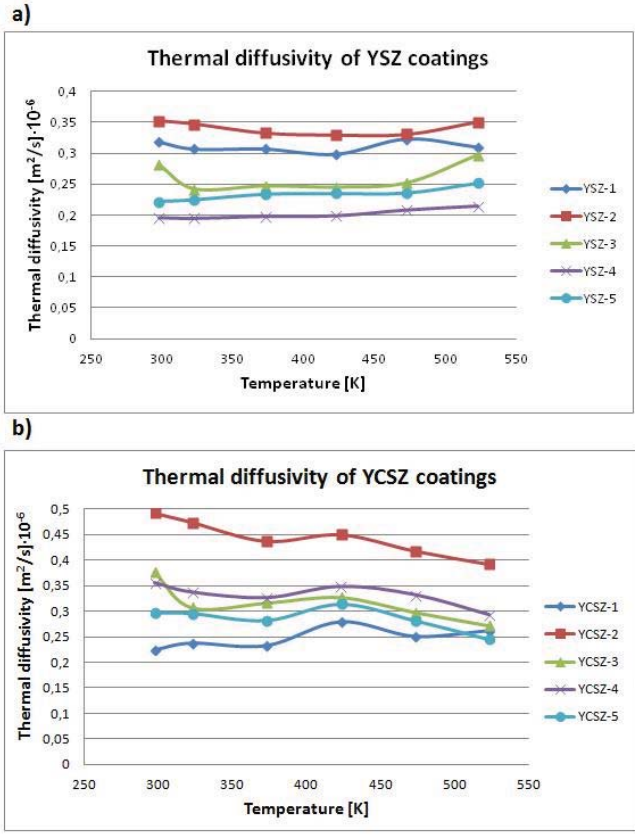

Fig. 4. Thermal diffusivity of (a) 8YSZ and (b) 24CeYSZ coatings [11, 12]

3.3 Thermal conductivity

Thermal conductivity values calculated following equation (1) and shown in Fig.5 were as follows:

- thermal conductivity values was in the range from 0.47 to 1.03 W/(m·K) for 8YSZ (Fig. 5a). The increase in thermal conductivity with temperature was found also for these coatings. The highest values were noted for the highest temperature of 523 K at which the measurements were performed.
- thermal conductivity values were from 0.46 to 1.07 W/(m·K) for 24CeYSZ coatings (Fig. 5b). The shape of the curves was slightly more constant with temperature than that of 8YSZ coatings.

4 Discussion

The optimization of the milling parameters allowed obtaining powders with very small diameter for both 8YSZ as well as 24CeYSZ. The use of liquid feedstock being a suspension of submicrometric solids and plasma spraying method enabled to obtain the coatings with finely grained microstructure. This type of structure is difficult to achieve with standard atmospheric plasma spraying (APS) working with dry feedstock. The APS coatings have bigger lamellae and do not have very fine grains [13]. SEM observation enabled to find that 8YSZ coatings showed more of well molten lamellae and smaller amount of fine sintered powder particles than 24CeYSZ coatings. The total porosity and number of microcracks of 8 YSZ coatings is also lower.The porosity of the 8YSZ coatings depends on spray parameters, namely, increases with the spray distance. The 24CeYSZ coatings did not show such correlation. Moreover greater number of cracks in the 24CeYSZ coatings may be a result of slightly higher deposition temperatures, which have been noted during spraying process. The greater heat flux introduced into coating during its build up was probably associated with the generation of higher thermal stresses during the cooling of samples.
It was observed that the values of thermal diffusivity and thermal conductivity of the 8YSZ and 24CeYSZ coatings decrease of their porosity. The only one exception is 24CeYSZ coating sprayed in the run no. 4. However, in spite of higher porosity of 24CeYSZ coatings they do not show lower values of thermal transport properties than 8YSZ ones. A lot of studies have been carried out, which aimed to determine the effect of microstructure, especially porosity, on the thermal properties of zirconia coatings used as thermal barriers. Raghavan et al. [14] proved that the increase of the micro-porosity in the coating's results in a decrease in thermal conductivity values. On the other hand Carpio et al. [15] did not find a clear relationship between the porosity and thermal conductivity value. Apparently this issue still requires more research.

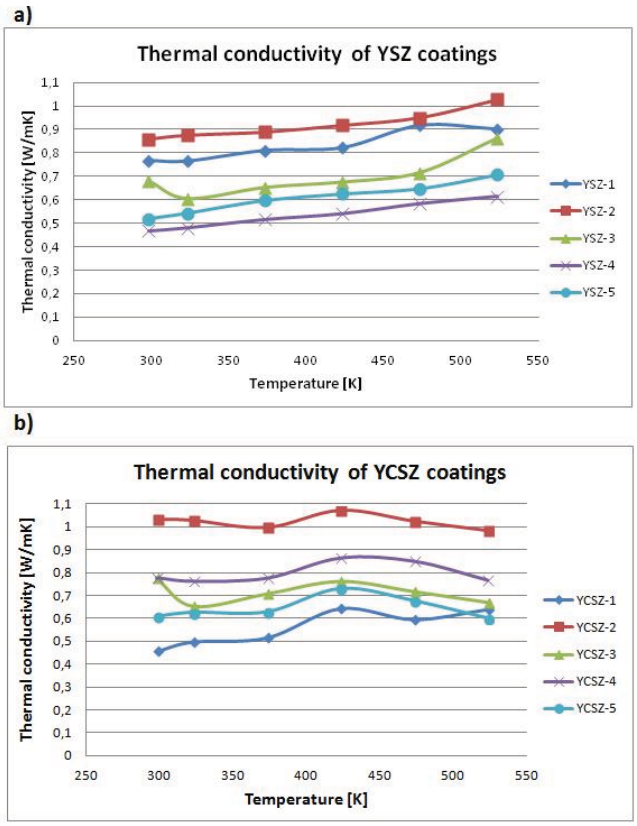

Fig.5. Thermal conductivity of (a) 8YSZ and (b) 24CeYSZ coatings [11, 12]

Conclusionq

Microstructure and thermal transport properties of two kinds of zirconia coatings 8(YSZ and 24CeYSZ) deposited by suspension plasma spraying method were investigated in this paper. The powders and suspensions were prepared and characterized. The powders had to been milled because of their great initial size. It allowed obtaining finely grained particles of powders with mean size equal to: d_{vs}=4.5µm (8YSZ) and d_{vs}=3.9 µm (24CeYSZ). The suspensions were formulated with the use of 40 wt. % of water, 40 wt. % of ethanol and of 20 wt. % of zirconia powder. The coatings were sprayed with similar operational parameters, where the variables were torch scan velocity and spraying distance. SEM microscopes and X-ray diffractometers were used to characterize microstructure of coatings. 8YSZ coatings showed porosity in the range of 8-12%, whereas the 24CeYSZ coatings porosity was in the range of 15-22%. The main phase in both cases was tetragonal ZrO_2 (at least 89% for YSZ and at least 95% for YCSZ). The measurements of thermal diffusivity were conducted with the use of laser flash method. The values of thermal diffusivity were similar for 8YSZ and 24CeYSZ coatings (approximately in the range of 0.2–0.5x10^{-6} m^2/s) and allowed calculate thermal conductivity. The values of thermal conductivity were relatively low for both 8YSZ (0.47 to 1.03 W/(m·K)) as well as 24CeYSZ (0.46 to 1.07 W/(m·K)). In the next studies, thermal properties measurements at higher temperatures and also thermomechanical properties tests, especially for YCSZ coatings, are planned.

Literature

[1] Gitzhofer F., Bouyer E., Boulos M.I., Suspension plasma spraying, US Patent 5 609 921, 3 November 1997

[2] Pawłowski L., The Science and Engineering of Thermal Spray Coatings: Second Edition, J. Wiley & sons, 2nd ed. 2008

[3] C. Delbos, J. Fazilleau, et al., Phenomena Involved in Suspension Plasma Spraying Part 2: Zirconia Particle Treatment and Coating Formation, Plasma Chemistry and Plasma Processing, Volume 26 (2006), Issue 4, pp. 393-414

[4] Fauchais P., Etchart-Salas R., et al., Parameters controlling liquid plasma spraying: solutions, sols or suspensions, Journal of Thermal Spray Technology, 17 (2008), pp. 31-59

[5] American Ceramic Society, Progress in Thermal Barrier Coatings, John Wiley & Sons, cop. 2009

[6] Łatka L., Investigation of ceramic coatings obtaned by suspension plasma spraying, Ph.D. Thesis, Wroclaw University of Technology and University Lille 1, 2012.

[7] http://imagej.nih.gov/ij/, consulted on 2 February 2014

[8] Cowan R.D., Pulse Method of Measuring Thermal Diffusivity at High Temperatures, Journal of Applied Physics, 34 (4) (1963), 926

[9] Pankratz L.B., Thermodynamic Properties of Elements and Oxides, U. S. Bureau of Mines Bulletin (1982), 672

[10] Takeda Y., Tu H.Y., Sakaki H., Imanishi N., Yamamoto O., Philips M.B., Sommes N.M., Gd1-xAxMnO3 (A = Ca and Sr) for the electrode of solid oxide fuel cells, Journal of The Electrochemical Society, 144 (1997), pp. 2810-2816.

[11] Łatka L., Cattini A., et al., Thermal diffusivity and conductivity of yttria stabilized zirconia coatings obtained by suspension plasma spraying, Surface & Coatings Technology, 208 (2012), pp. 87–91

[12] Sokołowski P., Łatka L., et al., Characterization of microstructure and thermal properties of YCSZ coatings obtained by suspension plasma spraying, published in 6RIPT conference in Limoges (2013), to be submitted on Surface and Coatings Technology

[13] Xing Y.-Z., Li C.-X., et al., Microstructure development of plasma-sprayed yttria-stabilized zirconia and its effect on electrical conductivity, Solid State Ionics 179 (2008), pp. 1483–1485

[14] Raghavan S., Wang H., et al., The effect of grain size, porosity and yttria content on the thermal conductivity of nanocrystalline zirconia, Scripta Materialia, vol. 39 (1998), no. 8, pp. 1119-1125

[15] Carpio P., Blochet Q., et al., Correlation of thermal conductivity of suspension plasma sprayed yttria stabilized zirconia coatings with some microstructural effects, Materials Letters 107 (2013), pp. 370–373